

Master Degree Project in Applied Microbiology



LUND
UNIVERSITY

Energy & redox fluxes in *Lactobacillus reuteri* DSM 17938 on different sugars

Master's programme in Biotechnology

Student

Katarzyna Bengtsson

Examiner

Ed van Niel

Supervisor

Christer Larsson

Lund University 2019

Summary

Under anaerobic condition the specific growth rate of *Lactobacillus reuteri* DSM 17938 on different sugars, was analyzed using spectrophotometry. Electron acceptor (fructose) supported cells to cope with poor energy recovery by re-oxidising the NADH, thus enabling ATP formation thru acetate production, while fermenting glucose via the phosphoketolase pathway (PKP) and simultaneously operating via Embden-Meyerhof pathway (EMP). The specific growth rate on glucose, maltose and sucrose was improved unquestionably in the presence of fructose.

Analysis of the fermentation products showed in the fermentations without fructose produced relatively more ethanol than in all other cases studied so far with *L. reuteri* DSM 17938. It indicated that the enzyme pyruvate dehydrogenase (PDH) is active. It can be hypothesized that the particular growth environment (SD4 without electron acceptor) caused intracellular conditions that activated PDH. Comparison with the literature revealed that this enzyme is highly regulated on metabolic level by a number of metabolites.

In short, this study displayed that the environmental conditions (anaerobic, pH 5.5) together with medium composition (SD4) had an effect of the fluxes through the two central carbon pathways in *L. reuteri* DSM 17938, which had no apparent effect on the energy and redox fluxes. Due to that ethanol could be produced via each pathway it made it impossible to estimate the flux in each pathway. Therefore, two extreme cases, regarding the variation in the cofactor formation flux ratio, RJ (ratio between the redox formation flux ($J_{\text{NADH+NADPH}}$), and the energy carrier formation flux (J_{ATP})), were investigated: PDH not active (SD4 media with e^- acceptor) and PDH active (SD4 media without e^- acceptor). The real case is somewhere between the two cases. Thus the results need verification and further experiments.

Additionally the data obtained from osmotic potential measurements reflected the product formed during the fermentation and showed linear correlation between osmotic potential and optical density.

Introduction and aim.....	5
Scientific background	6
<i>Lactobacillus reuteri</i> DSM 17938	6
Factors affecting the maximum growth rate	6
The genetic background of the cell.....	6
Temperature and pH	7
Media composition	7
Substrate uptake mechanism	8
Metabolic pathways	9
Product Flux and NAD(P)H/ATP Formation Flux Ratio	10
Work flow chart.....	11
Material and Methods	11
Batch fermentation.....	11
Optical density	11
Osmotic potential	11
HPLC.....	12
Enzyme activity assay of Pyruvate dehydrogenase (PDH).....	12
Standard method.....	12
PMS-MTT assay.....	12
Product fluxes	12
Cofactor formation flux ratio (R_c)	12
Results and discussion.....	13
Batch fermentation on different sugars.....	13
Osmotic potential	15
Energy and redox fluxes	17
Conclusions.....	22
Future recommendation	23
References.....	24
Appendixes	26
Appendix 1 Metabolic pathways with energy and redox ratios	26
Appendix 2 Excel data sheet.....	27
Appendix 3 Raw data.....	27

Introduction and aim

Human have billions of bacteria in their gut with 300 to 500 different kinds of species (Canny et al, 2008). Each and one of us has their own fingerprint of microbiota. The mix of bacteria in our body is determined by our mother's microbiota, the environment that we are exposed to at birth, our diet and lifestyle. The bacteria residence almost whole of our body, but the ones in our gut may have the biggest impact on our entire digestive system, and thus our well-being. *Lactobacillus reuteri* is one of the species that is resident in the gut (Molin 2013).

L. reuteri DSM 17938 was isolated from breast milk in 1990 and used in BioGaia's probiotic products ever since (BioGaia home page).

"Probiotics are live microorganism which when administered in adequate amounts confer a health benefits on the host " (Anon, 2002).

The probiotic market exceeded 36 billion USD in 2016 and is expected to reach revenues of 74 billion USD in 2024 (Grand View Research Inc. 2018).

This Master thesis is a part of the project work at Microbiology department at Lund's University and SLU (Uppsala), project by order of probiotic producing company BioGaia. This Master thesis is conducted to investigate the growth and behavior of *L. reuteri* DSM 17938 on different sugars.

The aim is to gain results on the growth rate, osmotic potential, energy and redox fluxes in *L. reuteri* DSM 17938 when growing on different sugars.

Scientific background

Lactobacillus reuteri DSM 17938

L. reuteri is a gram-positive, lactic acid bacterium that belongs to the heterofermentative lactobacilli group. Picture (Fig. 1) was taken after the fermentation of *L. reuteri* DSM 17938 (during the Probiotic project work), the average cell size was estimated to be 3 µm in length and 1 µm wide.



Figure 1. *L. reuteri* DSM 17938 under microscope, stationary phase, pH 5.5. Photo taken by K. Bengtsson.

This species is one of the most clinically studied probiotic species and is used in BioGaia products. Most of the conducted studies show strong clinically proven effects on children and infants. This strain has been shown to work in both therapeutic and preventive settings against acute diarrhea in children between the ages of 3 and 60 months (Urbańska et al., 2016; Gutierrez-Castrellon et al., 2014; Weizman et al., 2005). Supplementation of the diet with strain DSM 17938 can also reduce gastrointestinal tract symptoms (constipation and regurgitation) and improve colicky symptoms (reduce crying time) in breastfed infants (Sung et al., 2017; Indrio et al., 2014; Savino et al., 2010). Gastral tract diseases and infant colic can be connected to a leaky gut (increased intestinal permeability), and permeability can be reduced or even normalised using probiotic bacteria and compounds produced by these bacteria (Pallin, 2018).

Survivability is a key to a successful life-cells product. The latest scientific study investigated the impact of pH (4.5 - 6.5) and temperature (32 – 37 °C) on the stress resilience of *L. reuteri* DSM 17938 during freeze-drying and post freeze-drying exposure to low pH (pH 2) and bile salts and showed that pre-stressing at higher pH increase bacterial survival during freeze drying (Hernández et al. 2019).

Factors affecting the maximum growth rate

The genetic background of the cell

The characteristics of each species are important factors determining the growth rate. In general, the specific growth rate is lower the higher cells in the evolutionary scale:

E. coli > yeast > molds > animal cells

Temperature and pH

Both parameters depend on the organism preferences, for *E.coli* optimal temperature interval is 20 -37°C. Temperature and maximum growth dependence is approximated by the Arrhenius plot:

$$\mu_{max} = Ae^{-\Delta E/RT}$$

A - an organism-dependent constant

ΔE - the activation energy

R - the gas constant (J/mol, °K), (Larsson 2013)

Media composition

There are three principal media categories: minimal medium, complex medium and defined medium.

A minimal medium is based on very few simple components, usually only salts and a sugar.

A complex medium is commercial complex medium and less well defined. One example is the De Man, Rogosa and Sharpe agar (MRS), a selective culture medium designed for dense growth of Lactobacilli for lab studies.

A defined medium composed of carefully chosen and well defined components such as: salts, casamino acids, trace elements, amino acids, vitamins. One example is semi defined media SD4.

Most important component is a carbon source – sugar (glucose, maltose, sucrose).

During the anaerobic fermentation the fructose can be used not only as a carbon source but also an electron acceptor.

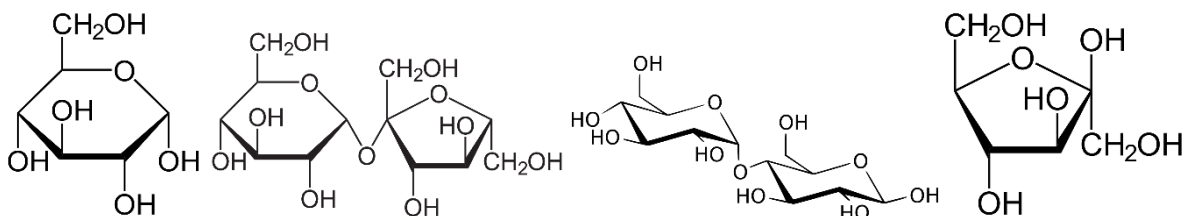


Figure 2. Sugars (from left to right): Glucose, Maltose, Sucrose, Fructose (electron acceptor). Figures copied from Wikipedia.

All organisms obtain energy by transferring electrons from an electron donor to an electron acceptor. During this process the electron acceptor is reduced and the electron donor is oxidized (Microbiology, 2002).

In the anaerobic fermentation (as performed in this study) there is no oxygen serving as an electron acceptor. For *L. reuteri* pyruvate and acetyl-CoA function as the final electron acceptors which end up in the production of lactate and ethanol, respectively. In addition, when present in the medium, fructose is also used as an electron acceptor resulting in mannitol as the end product (Figure 3). In all these steps NADH is reoxidized to NAD⁺.



Figure 3. Oxidation of NADH to NAD⁺ when fructose is converted to mannitol. Created by K. Bengtsson.

Substrate uptake mechanism

Diffusion

Small molecules (salt or oxygen) are taken up into the cell through the diffusion channels, substrate uptake is linear. Uptake can be expressed by:

$$v = \frac{k[s]}{\text{membrane area}}$$

v- uptake rate, k-permeability coefficient (Larsson 2013)

Uptake through specific transporters (carriers)

Bigger molecules such as sugars can be hydrolyzed outside the cell and taken up through the glucose transporters or can be transported directly into the cell by specific transporters. Uptake can be expressed by:

$$q_s = q_{max} \frac{s}{k_s + s}$$

q_s- specific uptake rate, k_s- substrate saturation constant (Larsson 2013)

Bigger molecules such as sugars can be hydrolyzed outside the cell and taken up into the cell by specific transporters. *L. reuteri* has putative transport proteins which are located in an operon specific for the substrate. Transporters for glucose, maltose and sucrose were found and are annotated as follows: ScrT: D-sucrose transporter; MalT: D-maltose transporter; GlucU/GlucU1/GlucU2: D-glucose transporters (Figure 4, Zhao et al, 2018).

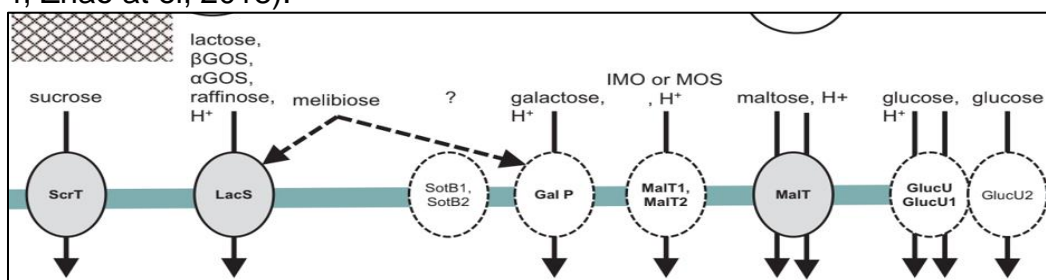


Figure 4. Overview of carbohydrate transport in *L. reuteri*. Copied from (Zhao et al, 2018).

Metabolic pathways

Homofermentative lactic acid bacteria use the Embden-Meyerhof pathway (EMP) to generate lactate as the only product of fermentation. Heterofermentative lactic acid bacteria use the phosphoketolase pathway (PKP) to produce: carbon dioxide, ethanol, acetate and lactate (Microbiology, 2002).

Work done by Årsköld et al., 2008 present that *L. reuteri* uses the PKP and EMP simultaneously.

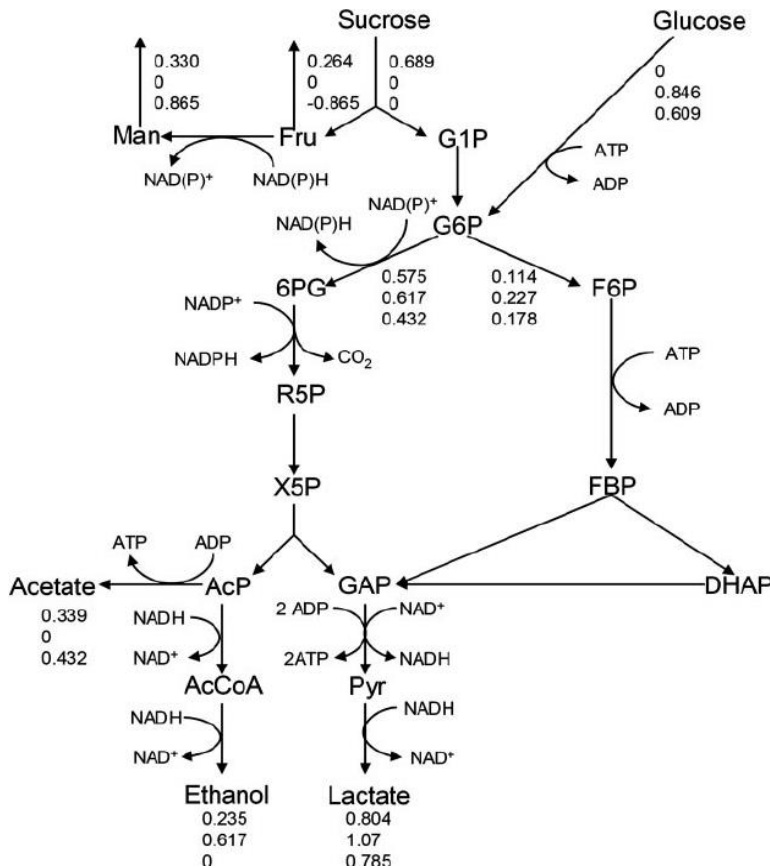


Figure 5. Pathways of sucrose and glucose metabolism in *L. reuteri* ATCC 55730 as proposed by the metabolic flux analysis, annotated genome sequence, and in vitro enzyme assays. The fluxes (mol·mol biomass⁻¹·h⁻¹) represent those of cultures on 50 g·liter⁻¹ sucrose, 50 g·liter⁻¹ glucose, and 25 g·liter⁻¹ glucose plus 25 g·liter⁻¹ fructose. Fru, fructose; Man, mannitol; G1P, glucose-1-phosphate; G6P, glucose-6-phosphate; 6PG, 6-phosphogluconate; R5P, ribulose-5-phosphate; X5P, xylulose-5-phosphate; AcP, acetyl phosphate; AcCoA, acetyl coenzyme A; F6P, fructose-6-phosphate; FBP, fructose-1,6-bisphosphate; DHAP, dihydroxyacetone phosphate; GAP, glyceraldehyde-3-phosphate; Pyr, pyruvate. Copied from (Årsköld et al., 2008).

Product Flux and NAD(P)H/ATP Formation Flux Ratio

L. reuteri obtains ATP only through substrate level phosphorylation as they do not possess a complete electron transport chain to carry out oxidative phosphorylation. In the latter NADH is reoxidized with oxygen or nitrate as electron acceptors. Instead, in *L. reuteri* NADH is reoxidized with use of an intracellular organic molecule such as pyruvate or AcCoA. This will lead to the production of lactate and ethanol. Usually, in most anaerobic microorganisms the redox metabolism (NAD(P)H production) and energy metabolism (ATP production) are in balance, but this is not so in *L. reuteri*. In this organism relatively more redox carriers (NAD(P)H) are produced than energy carriers (ATP). To put a value on this we have to look at the formation fluxes of both types of carriers.

In fermentation process product (ethanol, acetate, lactate) formation flux (J) can be defined as follows:

$$\text{FLUX (J)} = \text{Slope concentration/OD} \quad (\text{mM/ OD}) \times \mu_{\max}$$

When the product flux is combined with formation of NADH and ATP in the metabolic pathway for the product, the dimensionless parameter - the cofactor formation flux ratio (R_J) can be introduced:

$$R_J = \frac{J_{\text{NAD(P)H}}}{J_{\text{ATP}}}$$

R_J is the ratio between the redox formation flux ($J_{\text{NADH+NADPH}}$), and the energy carrier formation flux (J_{ATP}) (van Niel et al, 2017). The relationship between the cofactor formation flux ratio and the normalized specific growth rate is presented in Figure 6.

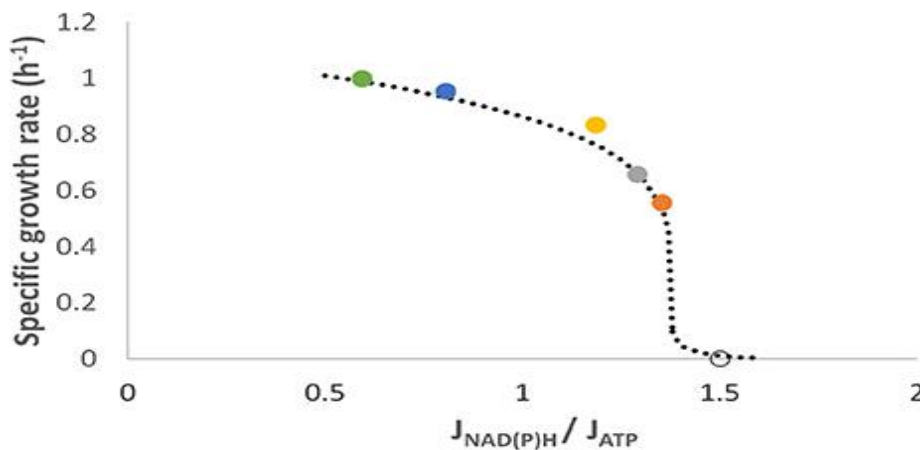


Figure 6. Relationship between the cofactor formation flux ratio and the normalized specific growth rate of various *L. reuteri* strains growing anaerobically. These data points were calculated from (left to right): (●) strain ATCC 55730 on sucrose (Årsköld et al., 2008), (●, ●) strain DSM 17938 on glucose (this study) and (●, ●) strain ATCC 55730 on glucose (this study). No growth (o) is assumed to be in the case there is zero flux through the EMP (100% flux through the PKP) and thus the R_J is equal to 1.5. Copied from (van Niel et al, 2017).

The R_J parameter can be used to describe the metabolic state of the cell under anaerobic growth, to reevaluate central carbon metabolisms in prokaryotes, as a novel analytical tool for targeted design of new strains (van Niel et al, 2017)

Work flow chart

Following work had been done on the *L. reuteri* DSM 17938.

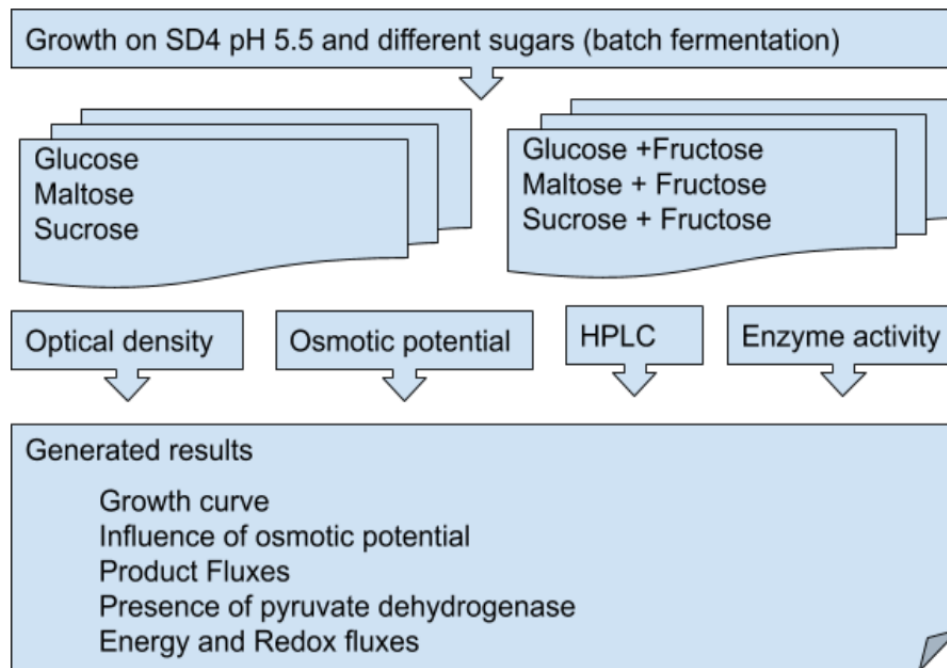


Figure 7. Work flow chart, outcome from master thesis, “Energy & redox fluxes in *Lactobacillus reuteri* DSM 17938 on different sugars”. Created by K. Bengtsson.

Material and Methods

Batch fermentation

L. reuteri strain DSM17938, obtained from BioGaia AB, Stockholm, Sweden, was inoculated in 10 ml MRS overnight at 37°C, washed in 45 ml PBS and double sample were grown under anaerobic conditions on glucose (25 g liter⁻¹), maltose (25 g liter⁻¹), sucrose (50 g liter⁻¹), glucose plus fructose (25 g liter⁻¹ each), maltose plus fructose (25 g liter⁻¹ each) and sucrose plus fructose (50 resp 25 g liter⁻¹) at 37°C and pH 5.5 using a semi defined medium (SD4). The pH was adjusted by automatic titration with 3 M KOH, and the stirring speed was set to 100 rpm. Nitrogen gas was sparged through the culture to create an anaerobic environment and was maintained by the production of carbon dioxide in the culture.

Optical density

OD was measured spectrophotometrically at 620 nm, at least once an hour during the whole cultivation. The least squares method was used using Excel (Microsoft 2013) to estimate maximal growth rate (μ_{max}) using the optical density data.

Osmotic potential

Osmolality (mili-osmol/kg H₂O), 100 ul centrifuged sample was measured with a Micro-Osmometer (Type DR-02) and is based on freezing point depression measurement. Supernatants were checked at least once an hour during the whole

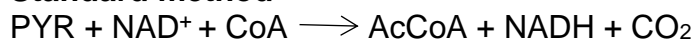
cultivation. Micro-Osmometer was calibrated with 300 mOsm standard and controlled with 0.9% NaCl before use (286 +/- 3 mOsm).

HPLC

The concentrations (g/L) of glucose, sucrose, maltose, fructose and fermentation products (acetate, ethanol and lactate) were determined by high-pressure liquid chromatography with IR-detector. Sugars and products were separated on a Rezex™ ROA-Organic Acid H+ (8%) ion exclusion column (H16-136289, Phenomenex), with 5 mM H₂SO₄ as the mobile phase (0.6 mL/min).

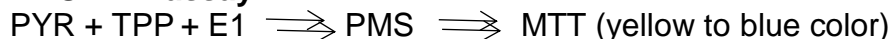
Enzyme activity assay of Pyruvate dehydrogenase (PDH)

Standard method



Continuous spectrophotometric rate determination, T=30°C, pH= 7.4, A_{340nm}
3 mL reaction mix, the final concentrations were: 51 mM MOPS, 0.20 mM magnesium chloride, 0.01 mM calcium chloride, 0.30 mM co-carboxylase, 0.12 mM coenzyme A, 0.2 mM B-NAD, 2.64 mM L-cysteine hydrochloride, 5.1 mM pyruvate and crude sample with PDH, (Brown, 1976). Beside the cysteine, both nitrogen and argon gas were used to create an anaerobic environment.

PMS-MTT assay



Continuous spectrophotometric rate determination, T=30°C, pH= 7.1, A_{560nm}
3 mL reaction mix, the final concentrations were: 50 mM potassium phosphate buffer (pH 7.1), 1 mM magnesium chloride, 0.2 mM TPP, 0.5 mM MTT, 6.5 mM PMS and 2 mM sodium pyruvate and crude sample with PDH, (Ke et al, 2014).

Product fluxes

Products concentrations (g/L) obtained from HPLC analysis were converted to mM (mmol/L) and plotted against optical density (OD at 620 nm), slopes gained were used for flux calculations. Exponential phase products (ethanol, acetate, lactate) formation fluxes (J) were determined with following formula:

$$\text{FLUX (J)} = \text{Slope (mmol /L/ OD)} \times \mu_{\text{max}}$$

Cofactor formation flux ratio (R_J)

R_J for different metabolic pathways were calculated, 1) for PKP and EMP pathways combined and 2) including the pyruvate dehydrogenase pathway and assuming that all ethanol is produced via the EMP pathway. See Appx 1 (Fig. 17&18) for metabolic pathways with energy and redox ratios.

$$1) \quad R_J = \frac{2J_{Ac} + 2J_{EtOH} + J_{Lac}}{J_{Ac} + 2J_{Lac}} \quad \text{Both PKP and EMP}$$

$$2) \quad R_J = \frac{2J_{Ac} + 2J_{EtOH} + J_{Lac}}{J_{Ac} + 2J_{EtOH} + 2J_{Lac}} \quad \text{EtOH formed via EMP}$$

Results and discussion

Batch fermentation on different sugars

The growth curves are the graphical representations of how the cell mass increases with time. Curves generated in this study (Fig. 8) demonstrated improved growth of *L. reuteri* DSM 17938 when the electron acceptor fructose was present in the medium. It took longest time to reach stationary phase with glucose only and fastest on sucrose and fructose. Curves showed also that strain DSM 17938 grown on glucose had higher biomass then the one grown on sucrose and fructose. It is clear that the carbon source affects the growth performance and it is important to consider this information when choosing the growth medium.

At the end of the fermentations cells were harvested and frozen until they will be used for determining their survivability after freeze drying at the Agriculture University of Sweden in Uppsala. Unfortunately, this part has not been carried out yet.

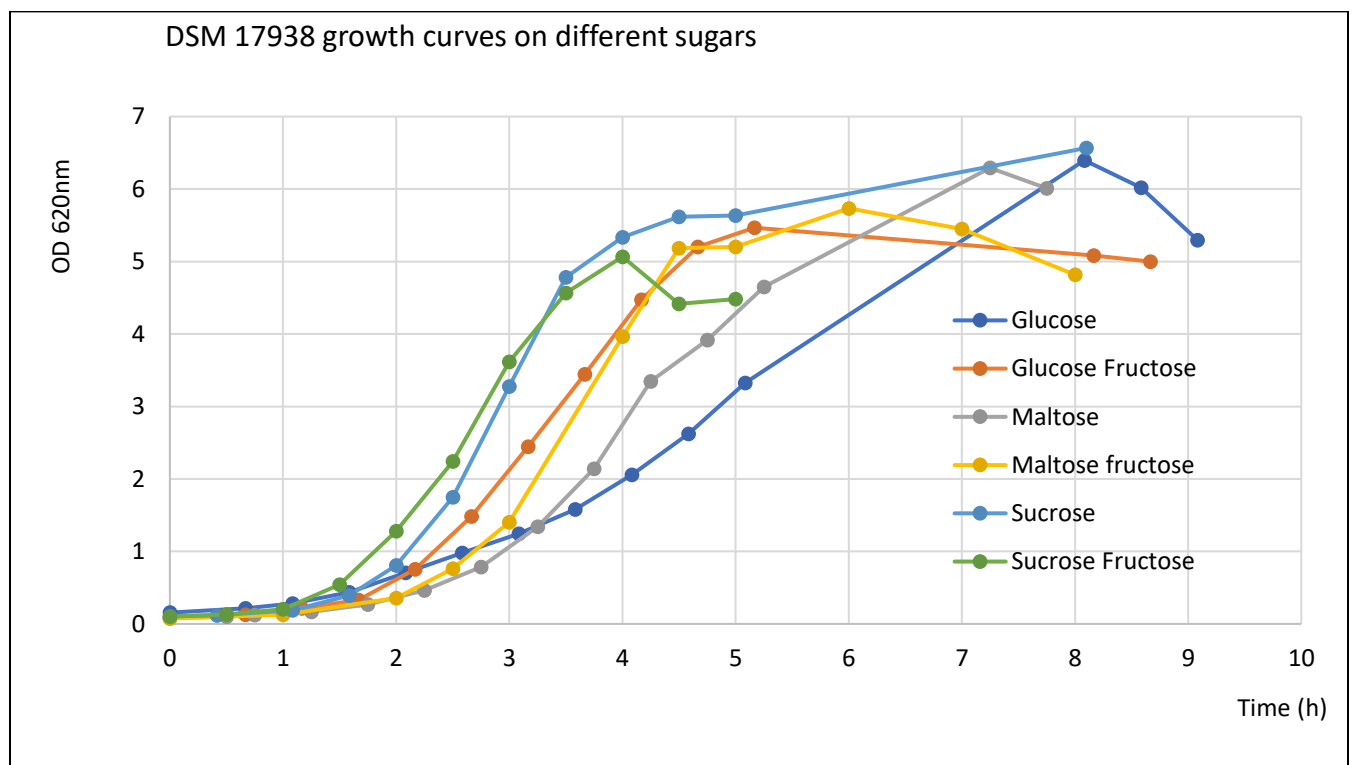


Figure 8. *L. reuteri* DSM 17938 growth curves on different sugars, with and without electron acceptor (fructose). Anaerobic fermentation, SD4 medium, pH 5.5, sugar corresponding to 25g/L of glucose concentration, fructose 25 g/L, OD 620nm.

Table 1. *L. reuteri* DSM 17938 on different sugars, with and without electron acceptor (fructose). Maximum specific growth rate (μ_{max} estimated with least squares method Excel), maximum OD value and standard deviation between double samples. Anaerobic fermentation, SD4 medium, pH 5.5, sugar corresponding to 25g/L of glucose concentration, fructose 25 g/L.

	μ_{max}	max OD	SD
Glucose	0.84	6.40	0.4478
Maltose	1.07	6.29	0.3653
Maltose Fructose	1.20	5.73	0.6128
Glucose Fructose	1.33	5.47	0.0471
Sucrose	1.51	5.62	0.2121
Sucrose Fructose	1.60	4.48	0.0236

Electron acceptor promoted growth and specific growth rate was the highest when grown on sucrose and fructose (Tab. 1 & Fig. 9). Sucrose (second best), as predicted, increased the growth rate, both due to presence of fructose in the molecule structure and to an efficient uptake by specific ScrT: D-sucrose transporter (Zhao et al, 2018).

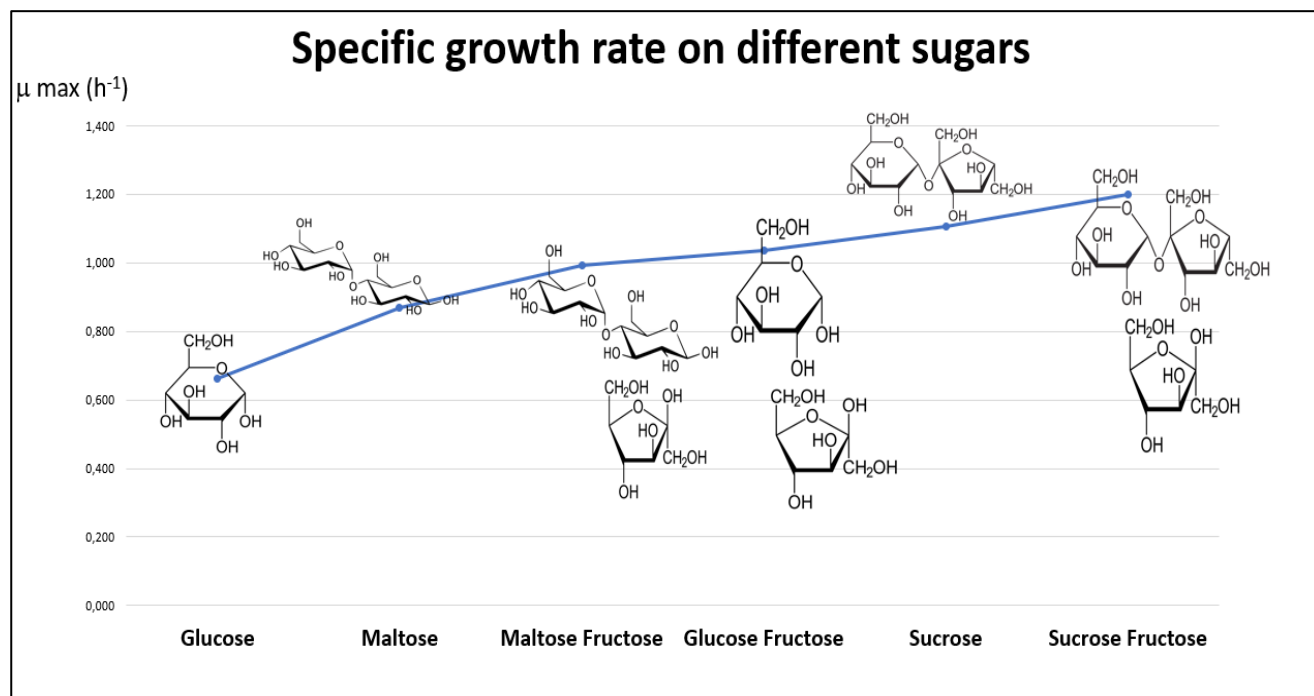


Figure 9. *L. reuteri* DSM 17938 specific growth rate on different sugars, with and without electron acceptor (fructose). Sugars molecular structures are presented. Anaerobic fermentation, SD4 medium, pH 5.5, sugar corresponding to 25g/l of glucose concentration, fructose 25 g/L, μ_{max} estimated with least squares method (Excel).

The electron acceptor increased the growth rate for all sugars used in this study: glucose, maltose and sucrose (Fig.10).

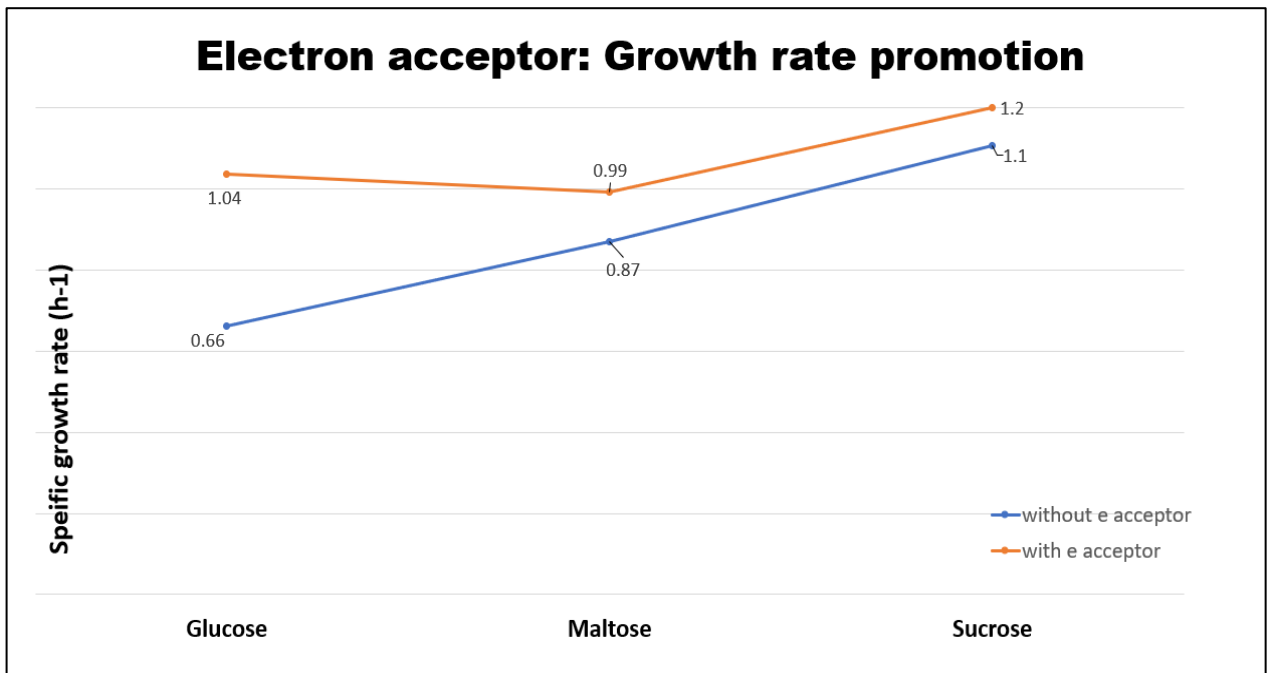


Figure 10. *L. reuteri* DSM 17938 specific growth rate on different sugars, with and without electron acceptor (fructose). Anaerobic fermentation, SD4 medium, pH 5.5, sugar corresponding to 25g/L of glucose concentration, fructose 25 g/L, μ_{max} estimated with least squares method (Excel).

Osmotic potential

The initial osmolality was higher on sucrose with electron acceptor (529 mOsm/kg H₂O) than on sucrose (336 mOsm/kg H₂O, Fig. 11), since the fructose was added to the medium on a same weight basis (25 g/L).

Osmolality followed the growth curve, constantly increasing with OD. As the osmolality is based on freezing point depression measurement and the freezing point depends on particles in solution, the osmolality increased with product formation even when OD decreased (Fig. 11). All cultures studied behaved in the same way, concerning the osmolality, as the representative shown in Fig. 11.

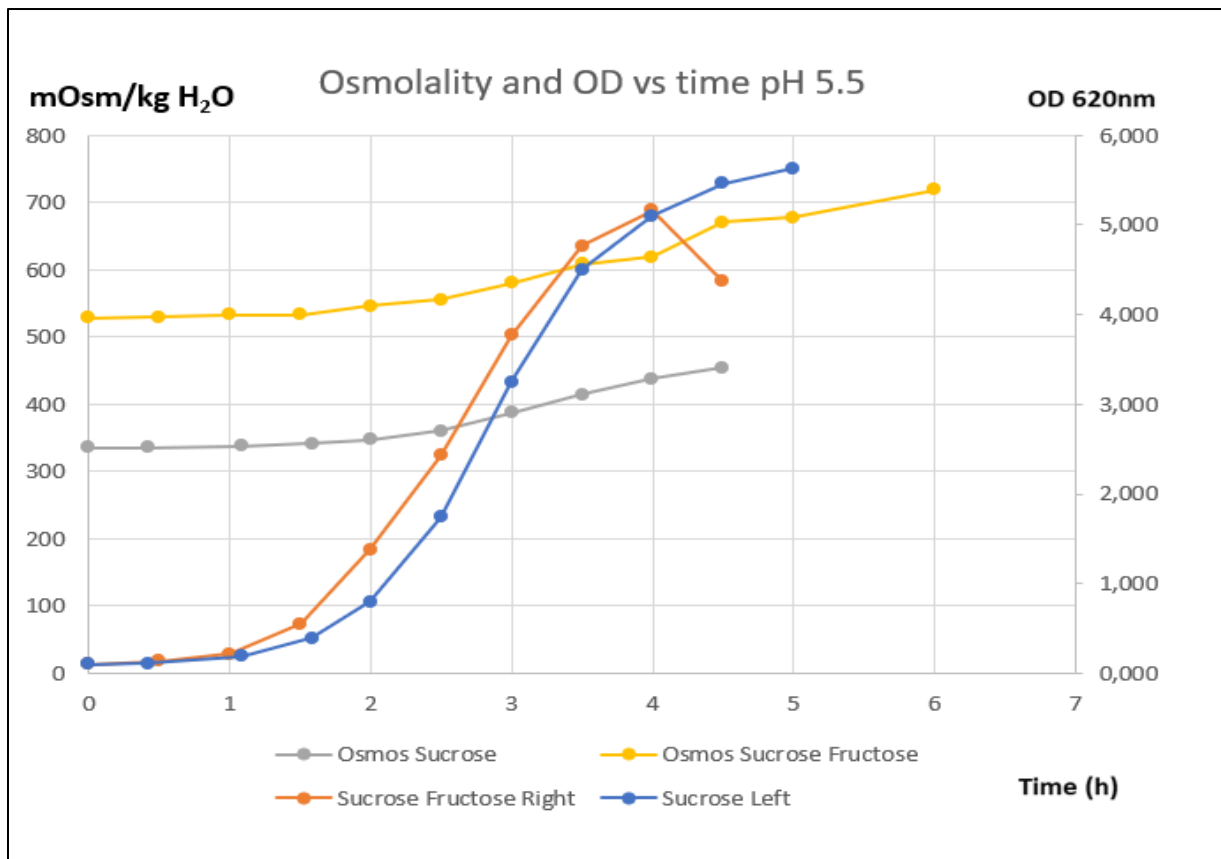


Figure 11. *L. reuteri* DSM 17938 on sucrose and sucrose and fructose. Growth curve vs time and osmolality vs time. Anaerobic fermentation, SD4 medium, pH 5.5, sugar corresponding to 25g/L of glucose concentration, fructose 25 g/L.

The osmotic pressure (Π) was linearly correlated to the optical density (OD) according to:

$$\Pi = \Delta\Pi \times OD + \Pi^0 \text{ (mOsm/kg H}_2\text{O)}$$

where $\Delta\Pi$ is the specific change of osmotic pressure during fermentation (mOsm/kg H₂O/OD) and Π^0 is the initial osmotic pressure measured at the start of the cultivation (mOsm/kg H₂O), (Willquist 2009).

A linear correlation (Fig. 12) was obtained for all the sugars and was independent of the presence of an electron acceptor.

Osmotically active substances such as alcohols (ethanol), sugars (mannitol, fructose), lipids, proteins increase the osmolality in the sample (Krahn et al, 2006). The slopes (Fig. 12) were higher for the sugars without electron acceptor (sucrose, glucose, maltose). This is due to the products formed during these fermentations. Of the products, ethanol was produced in higher amount for these sugars and possesses a relatively higher osmolality per molecule than the other products formed. It is not a coincidence that the same sugar- maltose generated the highest slope (34 mOsm/kg H₂O/OD) and also the highest flux for ethanol (8.3 (mM/OD) x h).

Osmolality vs OD plots, for growth phase showed the same pattern.

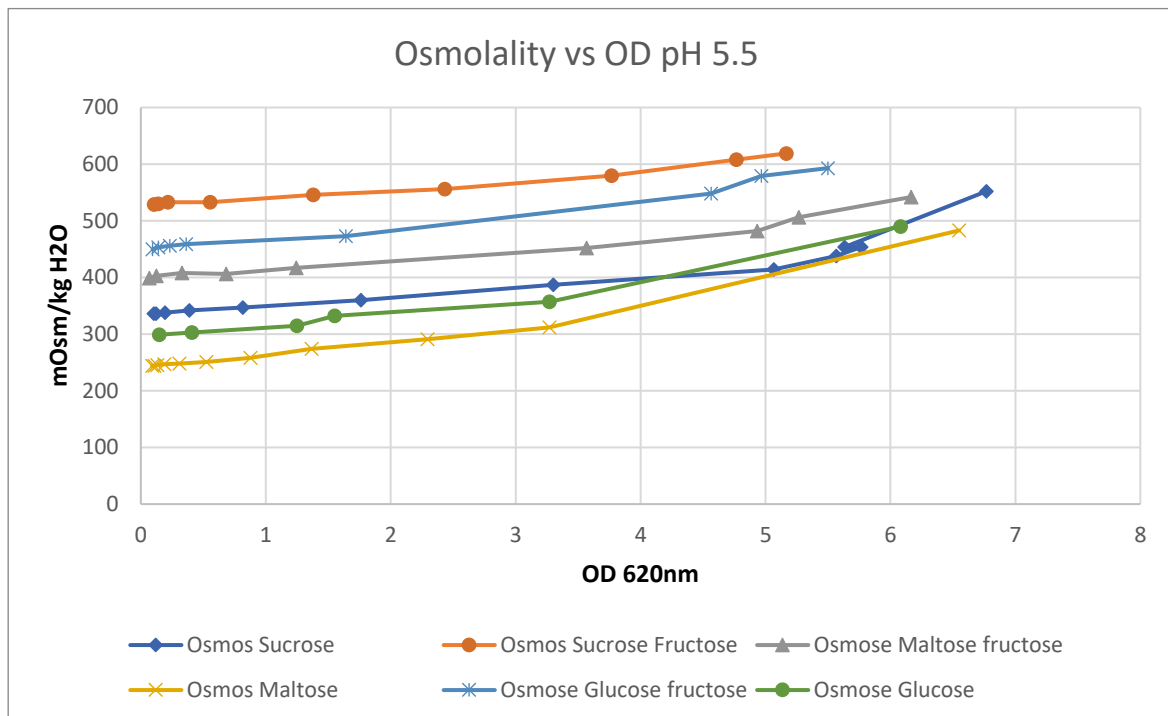


Figure 12. Linear correlation, osmolality to the optical density. *L. reuteri* DSM 17938 on different sugars. Anaerobic fermentation, SD4 medium, pH 5.5, sugar corresponding to 25g/L of glucose concentration, fructose 25 g/L.

Linear equation with slope and coefficient of determination R^2 (from the top down)

Sucrose fructose $y = 16.751x + 524.85$ $R^2 = 0.9729$

Glucose fructose $y = 25.221x + 446.21$ $R^2 = 0.9789$

Maltose fructose $y = 20.687x + 394.67$ $R^2 = 0.9553$

Sucrose $y = 23.847x + 325.99$ $R^2 = 0.873$

Glucose $y = 31.48x + 282.68$ $R^2 = 0.9494$

Maltose $y = 34.548x + 232.21$ $R^2 = 0.9502$

Energy and redox fluxes

Product fluxes (Table 2) during the exponential growth phase may reflect the pathways chosen by *L. reuteri* DSM 17938 during the fermentation.

As mentioned, the heterofermentative lactic acid bacteria use the PKP pathway to produce: ethanol, acetate and lactate in ratio 1:1 ($\text{Acet} + \text{EtOH} = \text{Lac}$), however, on sugars with electron acceptor, *L. reuteri* DSM 17938, clearly produced relatively more lactate in ratio 1: < 1 ($\text{Acet} + \text{EtOH} < \text{Lac}$).

The two simultaneously operating pathways PKP and EMP were active on sugar and electron acceptor. Some of the obtained results confirm work done by Årsköld et al, 2008.

In the anaerobic fermentation performed in this study fructose was the electron acceptor. Fructose was converted to mannitol, reoxidizing the NADH to NAD^+ and at the same time enabling the production of acetate, thus the flux through the acetaldehyde pathway could be relaxed to reoxidize the NADH, and consequently no ethanol was found. Acetate was found each time fructose was present in the medium and vice versa no acetate was found in the absence of fructose. It is important to

mention that on sucrose, acetate was formed due to the presence of fructose in the molecule structure of sucrose.

Results on sugars without electron acceptor revealed the possibility of a pathway normally not seen active in *L. reuteri* DSM 17938. For glucose, maltose and sucrose the sum of ethanol and acetate production was higher than lactate, or ratio 1:>1 (Acet+EtOH>Lac). Thus the stoichiometric ratio had changed, most probably through ethanol being produced via the additional pathway, containing pyruvate dehydrogenase (Fig. 13). This was not seen before in previous studies, but then the complex MRS medium was used whereas in the current study the lean SD4 was used throughout.

Table 2. Exponential phase product fluxes ((mM/OD) h) in *L. reuteri* DSM 17938 on different sugars. Anaerobic fermentation, SD4 medium, pH 5.5, sugar corresponding to 25g/L of glucose concentration, fructose 25 g/L.

	Lactate	Acetate	Ethanol	Acet+ EtOH	
SUGAR	FLUX (mM/OD) x h				
Glucose	4.919	0.000	7.038	7.038	
Glucose	4.999	0.000	6.328	6.328	EtOH + Ac > Lactate
Glucose Fructose	6.937	6.687	0.000	6.687	
Glucose Fructose	6.707	6.378	0.000	6.378	EtOH + Ac =/< Lactate
Maltose	6.326	0.000	8.291	8.291	
Maltose	5.681	0.000	7.020	7.020	EtOH + Ac > Lactate
Maltose Fructose	1.311	1.188	0.000	1.188	
Maltose Fructose	1.084	1.105	0.000	1.105	EtOH + Ac =/< Lactate
Sucrose	5.219	2.274	3.415	5.688	
Sucrose	4.725	1.868	3.625	5.493	EtOH + Ac > Lactate
Sucrose Fructose	2.818	1.900	0.000	1.900	
Sucrose Fructose	3.625	2.308	0.000	2.308	EtOH + Ac < Lactate

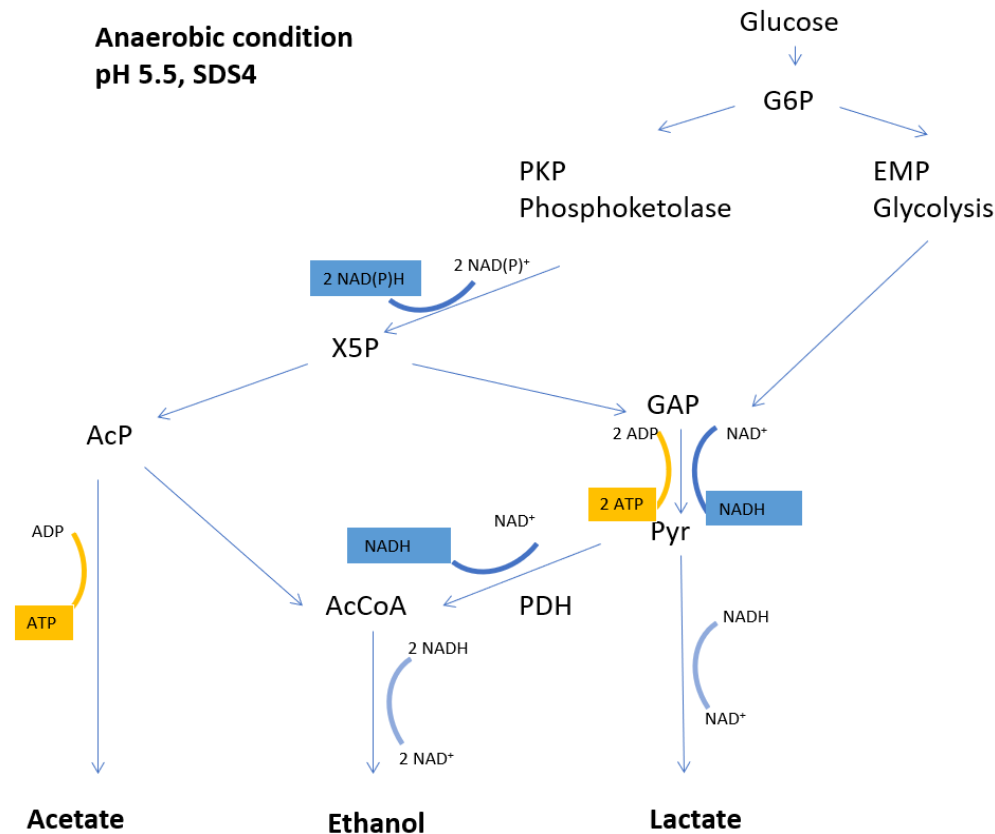


Figure 13. Pathways of glucose, maltose and sucrose metabolism in *L. reuteri* DSM 17938 as proposed by the metabolic flux analysis and annotated genome sequence. Pathways with NAD(P)H and ATP formation represent those of cultures on sugars corresponding to 25g/L of glucose concentration. Anaerobic fermentation, SD4 medium, pH 5.5. PKP phosphoketolase pathway, G6P, glucose-6-phosphate; X5P, xylulose-5-phosphate; AcP, acetyl phosphate; AcCoA, acetyl coenzyme A; EMP, Embden–Meyerhof–Parnas pathway; GAP, glyceraldehyde-3-phosphate; Pyr, pyruvate; PDH, pyruvate dehydrogenase. Created by K. Bengtsson.

Is the PDH pathway possible? There is evidence for the PDH presence in *L. reuteri*. An transcriptome analysis of *L. reuteri* ATCC 55730 (parental strain to *L. reuteri* DSM 17938) indicated that the PDH gen was significantly up-regulated (>1.5 fold, $P < 0.05$) in the early log phase. A Pan-metabolic model of *L. reuteri* ATCC 55730 and ATCC PTA 6475 based on whole genome sequences proved the presence of metabolic reaction: pyruvate to acetyl coenzyme A to ethanol (Pyr to AcCoA to EtOH) in *L. reuteri* ATCC 55730, but not in ATCC PTA 6475 (Saulnier et al. 2011). The gene *pdhA* encoding for the pyruvate dehydrogenase E1 component subunit alpha is present in *L. reuteri* DSM 20016, (UniProt, A5VJ72) .

The enzyme activity assays were conducted to prove PDH activity in the DSM strain, however, no results were obtained due to the crude sample, with other enzymes strongly interfering with the reactions. Purification of PDH is needed for successful monitoring of its activity and kinetics.

Pyruvate, CoA, NAD⁺, phosphoenolpyruvate PEP, adenosine monophosphate AMP, guanosine diphosphate GDP are known as PDH activators. NADH, AcCoA, CO₂ are known as PDH inhibitors (Goltschalk, 1979). It was found that the PDHc of *Escherichia coli* and *Lactococcus lactis* were active only at relatively low NADH/NAD ratios, (Snoep et al, 1993). High NADH/NAD ratios, associated with some substrates,

repress pdh expression, directly or indirectly (Cassey et al 1998). Rearranged results from Snoep et al, 1993 (Fig. 14) illustrate that a very small change in the presence of NADH in a substrate has a huge impact on the enzyme activity.

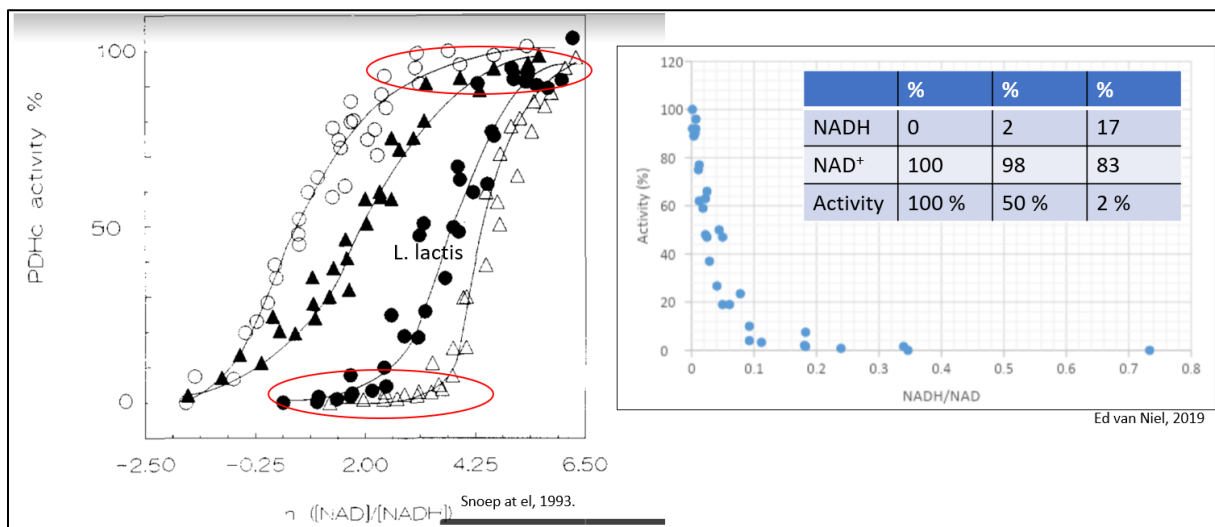


Figure 14. The effect of NADH/NAD ratio on the activity of the purified pyruvate dehydrogenase complexes (PDHc), results from Snoep et al, 1993 fig 1 rearranged by Ed van Niel.

Increased production of ethanol was not found on MRS cultivation. It is likely that MRS has a reducing effect on NAD⁺ creating a lower intracellular redox environment. In our study SD4 was used, the environmental conditions together with medium composition changed the pathway taken by *L. reuteri* DSM 17938, thus the product fluxes and the energy and redox fluxes, (Tab. 3 & 4). Two extreme cases can be investigated: PDH not active (SD4 media with e⁻ acceptor) and PDH active (SD4 media without e⁻ acceptor).

Table 3. R_J (J_{NADH+NADPH}) and specific growth (u_{max}) rate calculated for pathways of carbon metabolism in *L. reuteri* DSM 17938 as proposed by the metabolic flux analysis (Appx 1, 1) Fig.17) PKP and EMP pathways combined). The R_J represent those of cultures on sugars corresponding to 25g/L of glucose concentration and 25g/L fructose. Anaerobic fermentation, SD4 medium, pH 5.5.

J _{NAD(P)H} /J _{ATP}	Specific growth rate (h ⁻¹)	
1.833	0.662	Glucose
1.708	0.870	Maltose
1.347	1.106	Sucrose
0.987	0.993	Maltose Fructose
0.986	1.035	Glucose Fructose
0.870	1.200	Sucrose Fructose

Table 4. R_J ($J_{NADH+NADPH}$) and specific growth (μ_{max}) rate calculated for pathways of carbon metabolism in *L. reuteri* DSM 17938 as proposed by the metabolic flux analysis (Appx 1, 2) Fig.18) including the pyruvate dehydrogenase pathway, EtOH formed via EMP). The R_J represent those of cultures on sugars corresponding to 25g/L of glucose concentration and 25g/L fructose. Anaerobic fermentation, SD4 medium, pH 5.5.

$J_{NAD(P)H}/J_{ATP}$	Specific growth rate (h^{-1})	
0.987	0.993	Maltose Fructose
0.986	1.035	Glucose Fructose
0.870	1.200	Sucrose Fructose
0.848	1.106	Sucrose
0.784	0.662	Glucose
0.773	0.870	Maltose

Ethanol formation was only seen in the absence of any e^- acceptor, thus the expression of R_J ($J_{NADH+NADPH}$) were changed only for cultivation on glucose, maltose and sucrose. The R_J were reduced since the ethanol formation via EMP generated extra ATP (Appx 1, 2) Fig.18).

These were extreme cases and need further verification. The true values are in between the values obtained with these extreme cases.

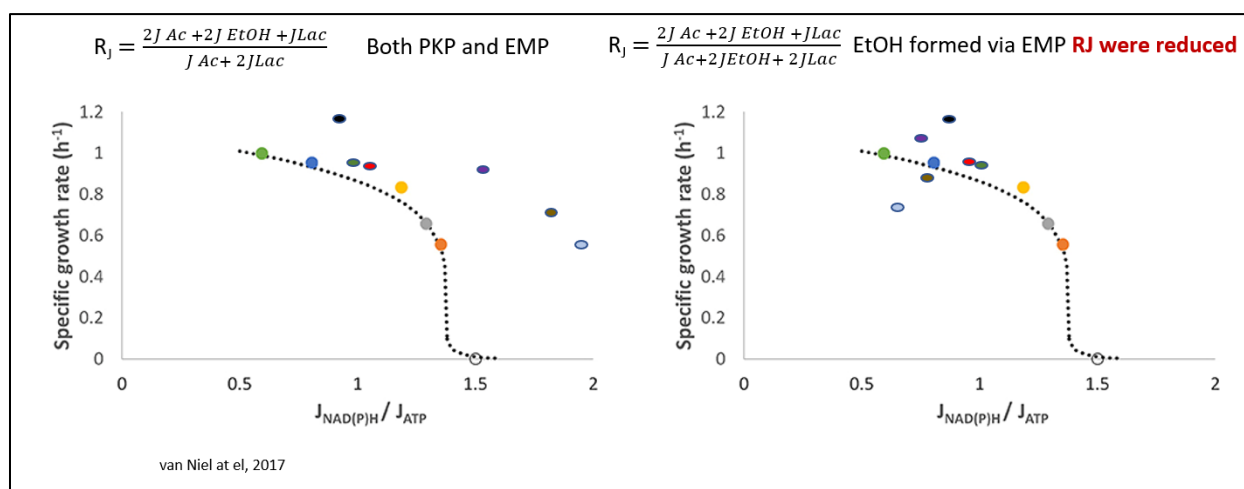


Figure 15. Relationship between the cofactor formation flux ratio and the normalized specific growth rate of various *L. reuteri* strains growing anaerobically. These data points were calculated from (left to right): (●) strain ATCC 55730 on sucrose (Årsköld et al., 2008), (●, ●) strain DSM 17938 on glucose (this study) and (●, ●) strain ATCC 55730 on glucose (this study). No growth (o) is assumed to be in the case there is zero flux through the EMP (100% flux through the PKP) and thus the R_J is equal to 1.5 (van Niel et al, 2017). Results from strain DSM 17938 table 3 and 4 were incorporated: (●) glucose, (●) maltose, (●) sucrose, (●) maltose fructose, (●) glucose fructose, (●) sucrose fructose.

Conclusions

The results gained during this study confirm the influence of the electron acceptor on the growth rate of *L. reuteri* DSM 17938. Under anaerobic fermentation, pH 5.5 and SD4 medium fructose is serving as electron acceptor and improves the growth rate on glucose, maltose and sucrose. The presence of an electron acceptor and its ability to reoxidize NADH enables also acetic acid production via the PKP. The osmotic potential based on freeze point depression reflects the product formation during fermentation and correlates linearly with the optical density.

The metabolic pathways can be changed under specific metabolic conditions, such as the NADH/NAD ratio. It is hypothesized that MRS, a commercial complex medium reduces the NAD⁺ and consequently increasing the NADH/NAD ratio. A high NADH/NAD ratio represses the PDH complex activity. It is further hypothesized that the SD4 medium creates a lower NADH/NAD ratio and thus activates PDH indirectly. The medium composition might also influence the concentrations of AMP, CoA, AcCoA and possibly other cofactors that have been found to control the rate of PHD in *E. coli* (Goltschalk, 1979). In other words, a similar complex control mechanism is foreseen in *L. reuteri*, and the influence of these compounds can be studied with purified PDH combined with a metabolomics study.

PDH activation opens a “new” pathway producing EtOH, and subsequently product formation fluxes change (Fig. 16).

Ethanol production via EMP and PDH generates ATP and reoxidises NADH, which is similar as for lactate production. Why might pyruvate conversion flux be directed to the PDH pathway and not lactate dehydrogenase (LDH)? It cannot be because of lactate being toxic for the cell as does ethanol. Maybe the goal is to create a higher flux of AcCoA, which is a hub metabolite within the metabolic network and thus might speed up biosynthesis.

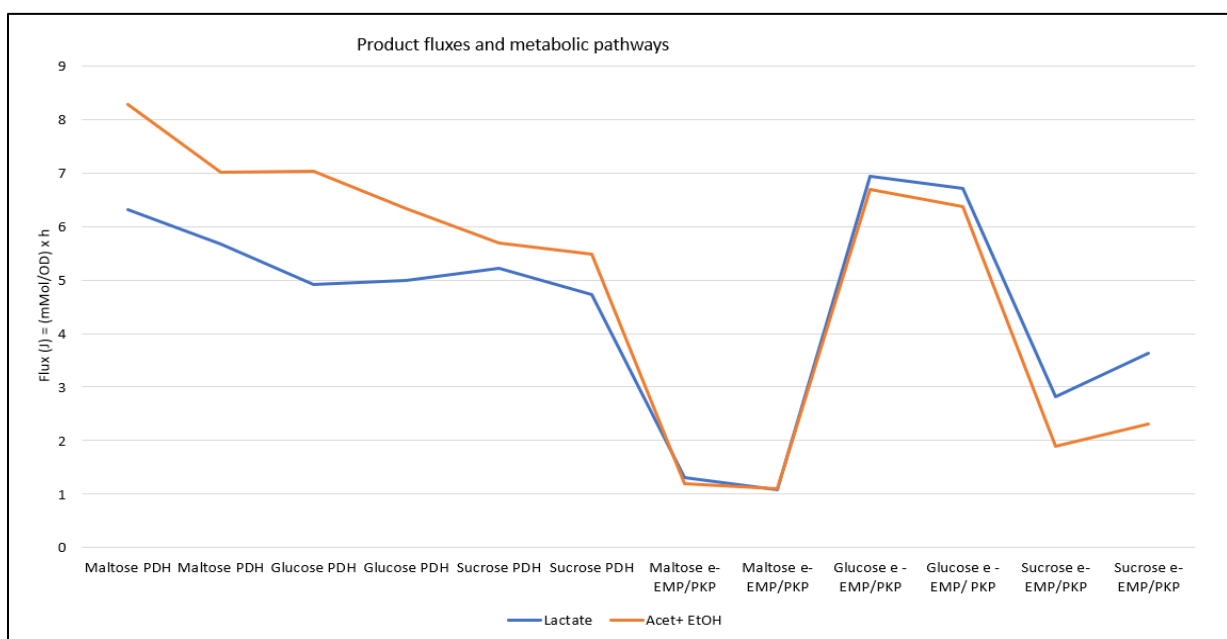


Figure 16. Metabolic pathways taken by *L. reuteri* DSM 17938, estimation based on product fluxes. Exponential phase product fluxes ((mM/OD) h) in *L. reuteri* DSM 17938 on different sugars. Anaerobic fermentation, SD4 medium, pH 5.5, sugar corresponding to 25 g/L of glucose concentration, fructose 25 g/L.

Future recommendation

Knock out of PDH to evaluate redox changes.

PDH enzyme activity method development regarding the extraction/purification of PDH from the crude sample.

Calculate the metabolic pathways ratio, to estimate the true pathway taken.

HPLC method development due to mannitol and fructose separation.

References

- Anon, (2002).** Joint FAO/WHO Working group report. *Guidelines for the Evaluation of Probiotics in Food*. London, Ontario, Canada.
- BioGia home page.** <https://www.biogaia.se>
- Brown, 1976.** Brown, J P., and Perham, R.N. 1976. *Biochem. J.* **155**, 419/247.
- Canny et al, 2008.** Geraldine O. Canny, Beth A. McCormick (2008) *Bacteria in the Intestine, Helpful Residents or Enemies from Within?* 10.1128/IAI.00187-08.
- Cassey et al 1998.** Cassey, B. (1998). Environmental control of pyruvate dehydrogenase complex expression in *Escherichia coli*. *FEMS Microbiology Letters*, **159(2)**, pp.325-329.
- G. Goltschalk, 1979.** Gerhard Gottschalk. 1979. *Bacterial Metabolism*. Boston: McGraw-Hill.
- Grand View Research Inc. 2018.** Grand View Research, Inc. (2018) *Probiotics Market*. In: Market estimates and trend analysis. <http://www.grandviewresearch.com/industry-analysis/probiotics-market>
- Hernández et al. 2019.** Armando Hernández, Christer Larsson, Radoslaw Sawicki, Ed W.J. van Niel, Stefan Roos, Sebastian Håkansson. *Impact of the fermentation parameters pH and temperature on stress resilience of Lactobacillus reuteri DSM 17938*.
- Ke et al, 2014.** Ke, C., He, Y., He, H., Yang, X., Li, R. and Yuan, J. (2014). A new spectrophotometric assay for measuring pyruvate dehydrogenase complex activity: a comparative evaluation. *Anal. Methods*, **6(16)**, pp.6381-6388.
- Krahn et al, 2006.** Krahn J, Khajuria A (April 2006). "Osmolality gaps: diagnostic accuracy and long-term variability". *Clin. Chem.* **52** (4): 737–9.
- Larsson 2013.** Gen Larsson. (KTH) Stockholm 2013. *Cultivation technology*.
- Microbiology, 2002.** Prescott, Lansing M., John P. Harley, and Donald A. Klein. 2002. *Microbiology*. Boston: McGraw-Hill.
- Molin, 2013.** Goran Molin. Lund 2013. Lectures in probiotics, *Physiologic and physiopathologic effects of the human microbiota*.
- Pallin, 2018.** Pallin, A., 2018. *Improving the functional properties of Lactobacillus reuteri* (Doctoral dissertation).
- Saulnier et al. 2011.** Saulnier, D., Santos, F., Roos, S., Mistretta, T., Spinler, J., Molenaar, D., Teusink, B. and Versalovic, J. (2011). Exploring Metabolic Pathway Reconstruction and Genome-Wide Expression Profiling in *Lactobacillus reuteri* to Define Functional Probiotic Features. *PLoS ONE*, **6(4)**, p.e18783.
- Savino et al., 2010.** Savino, F., Cordisco, L., Tarasco, V., Palumeri, E., Calabrese, R., Oggero, R., Roos, S. & Matteuzzi, D. (2010). *Lactobacillus reuteri DSM 17938 in infantile colic: a randomized, double-blind, placebo-controlled trial*. *Pediatrics*, **126(3)**, pp. e526-e533.

Snoep, et al 1993. Differences in sensitivity to NADH of purified pyruvate dehydrogenase complexes of *Enterococcus faecalis*, *Lactococcus lactis*, *Azotobacter vinelandii* and *Escherichia coli*: Implications for their activity in vivo. *FEMS Microbiology Letters*, **114**(3), pp.279-283.

Sung et al., 2017. Indrio et al., 2014. Sung, V., D'Amico, F., Cabana, M.D., Chau, K., Koren, G., Savino, F., Szajewska, H., Deshpande, G., Dupont, C. & Indrio, F. (2017). *Lactobacillus reuteri* to treat infant colic: a meta-analysis. *Pediatrics*, p. e20171811.

UniProt, Protein data bank. <https://www.uniprot.org>

Urbańska M et al, 2016. Urbańska M, Gieruszczak-Białek D, Szajewska H (2016) Systematic review with metaanalysis: *Lactobacillus reuteri* DSM 17938 for diarrhoeal diseases in children. *Aliment Pharmacol Ther* **43**:1025-1034

Wagner et al., 2005. Wagner, N., Tran, Q., Richter, H., Selzer, P. and Uden, G. (2005). Pyruvate Fermentation by *Oenococcus oeni* and *Leuconostoc mesenteroides* and Role of Pyruvate Dehydrogenase in Anaerobic Fermentation. *Applied and Environmental Microbiology*, **71**(9), pp.4966-4971.

van Niel et al, 2017. van Niel, E., Bergdahl, B. and Hahn-Hägerdal, B. (2017). Close to the Edge: Growth Restrained by the NAD(P)H/ATP Formation Flux Ratio. *Frontiers in Microbiology*, **8**.

Willquist 2009. Willquist, K., Claassen, P. and van Niel, E. (2009). Evaluation of the influence of CO₂ on hydrogen production by *Caldicellulosiruptor saccharolyticus*. *International Journal of Hydrogen Energy*, **34**(11), pp.4718-4726.

Zhao et al, 2018. Zhao, X. and Gänzle, M. (2018). Genetic and phenotypic analysis of carbohydrate metabolism and transport in *Lactobacillus reuteri*. *International Journal of Food Microbiology*, **272**, pp.12-21.

Årsköld et al., 2008. Årsköld, E., Lohmeier-Vogel, E., Cao, R., Roos, S., Radström, P. and van Niel, E. (2007). Phosphoketolase Pathway Dominates in *Lactobacillus reuteri* ATCC 55730 Containing Dual Pathways for Glycolysis. *Journal of Bacteriology*, **190**(1), pp.206-212.

Appendixes

Appendix 1 Metabolic pathways with energy and redox ratios

Cofactor formation flux ratio (R_j), 1) PKP and EMP pathways combined

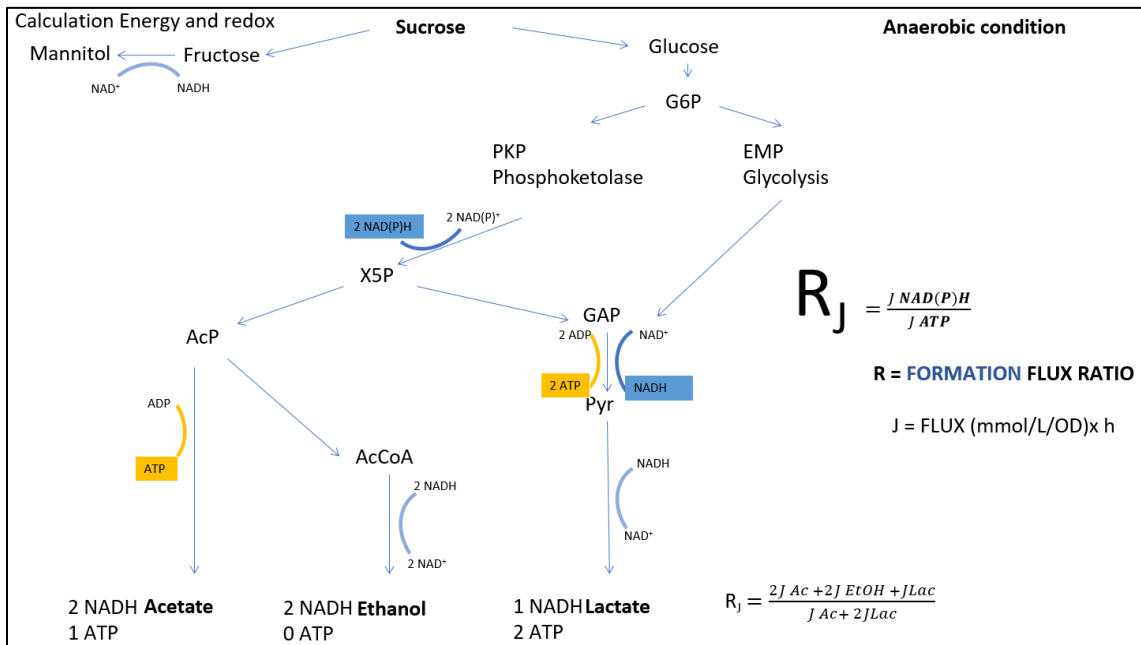


Figure 17. NAD(P)H and ATP formation flux ratio with metabolic pathways taken by *L. reuteri* DSM 17938, estimation based on product fluxes. Exponential phase product fluxes ((mM/OD) h) in *L. reuteri* DSM 17938 on different sugars. Anaerobic fermentation, SD4 medium, pH 5.5, sugar corresponding to 25 g/L of glucose concentration, fructose 25 g/L.

Cofactor formation flux ratio (R_j), 2) including the pyruvate dehydrogenase pathway

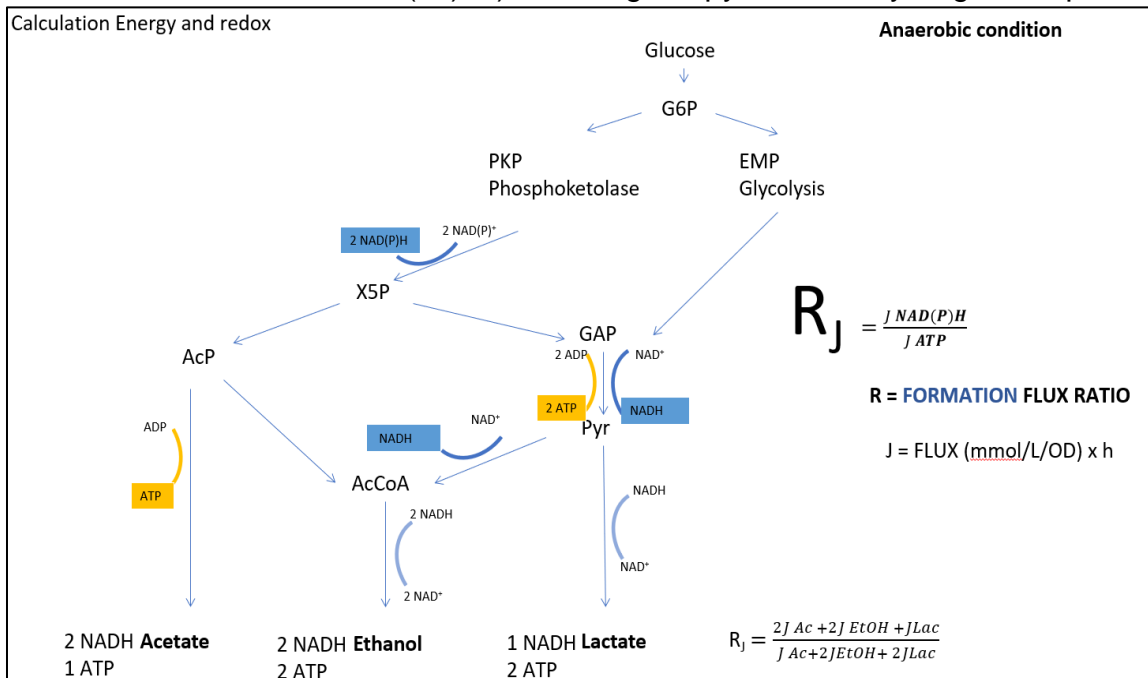


Figure 18. NAD(P)H and ATP formation flux ratio with metabolic pathways taken by *L. reuteri* DSM 17938, estimation based on product fluxes. Exponential phase product fluxes ((mM/OD) h) in *L. reuteri* DSM 17938 on different sugars. Anaerobic fermentation, SD4 medium, pH 5.5, sugar corresponding to 25 g/L of glucose concentration, electron acceptor (fructose) omitted.

Appendix 2 Excel data sheet

Excel data sheet "Energy end Redox fluxes in *L. reuteri* on different sugars", is included as a calculation and diagram source (contact author or examiner for the access).

Appendix 3 Raw data

12 fermentations, left and right (double sample), pH 5.5, SD4, anaerobic

Glucose Left

Glucose Right

Glucose Fructose Left

Glucose Fructose Right

Maltose Left

Maltose Right

Maltose Fructose Left

Maltose Fructose Right

Sucrose Left

Sucrose Right

Sucrose Fructose Left

Sucrose Fructose Right

F01863

LEFT

Batch code: G1L Batch type: pH 5.5 DSM 17938 Date: 20190206 Carbon source: Glucose
 Nitrogen source: - Sparging gas: - Stirrer speed: 100 Working volume: 1L
 GC sample code: _____ Operator: _____ Fermenter code: Applikon 1

Protocol	Date	Time		KOH mmol/l	Osmos %CO ₂	OD ₆₂₀				df	Abs OD ₆₂₀	Sample (ml)	Remark(s)
		Hour	Min			1	2	3	Ave.				
1			0	200	192	311	0.166	0.167	0.165				
2							0.232	0.234	0.229				
3				190		315	0.288	0.300	0.288	2			
4				187			0.251	0.257	0.255	10			
5				188			0.272	0.275	0.273	10			
6				188		330	0.104	0.107	0.101	10			
7							0.128	0.120	0.125	10			
8						337	0.160	0.157	0.165	10			
9				184			0.213	0.215	0.210	10			
10							0.269	0.275	0.275	10			
10							0.335	0.340	0.338	10			
10				182		374	0.038	0.039	0.032	100			
10				160		528	0.230	0.236	0.231	20			
10				156			0.154	0.147	0.150	40			
10				156		522	0.131	0.132	0.132	40			

F01863

RIGHT

Batch code: G2R Batch type: pH 5.5 DSM 17938 Date: 20190206 Carbon source: Glucose
 Nitrogen source: - Sparging gas: - Stirrer speed: 100 Working volume: 1L
 GC sample code: _____ Operator: _____ Fermenter code: Applikon 2

Protocol	Date	Time		KOH mmol/l	Osmos %CO ₂	OD ₆₂₀				df	Abs OD ₆₂₀	Sample (ml)	Remark(s)
		Hour	Min			1	2	3	Ave.				
11			0	50	45	299	0.145	0.147	0.146				
12							0.194	0.197	0.204				
12				43		303	0.263	0.266	0.263	2			
13				42			0.204	0.207	0.201	10			
14				42			0.088	0.086	0.090	10			
14				45			0.097	0.091	0.092	10			
15				41.5		315	0.122	0.118	0.125	10			
15						323	0.180	0.155	0.160	10			
16							0.197	0.190	0.203	10			
16				38			0.247	0.256	0.252	10			
17				32		357	0.332	0.323	0.326	10			
20				6→48		490	0.201	0.210	0.201	20			
20				45			0.149	0.156	0.147	40			
21				44.5		503	0.130	0.132	0.133	40			

Forsik 5 LEFT

Batch code: ML Batch type: DSM17938 pH 5.5 Date: 20190219 Carbon source: Maltose
 Nitrogen source: - Sparging gas: - Stirrer speed: 100 Working volume: 1L
 GC sample code: - Operator: Koro Fermenter code: Applikon 1

Protocol	Date	Time		%w/v KOH	%CO ₂ Osmos	OD ₆₀₀				df	Abs OD ₆₀₀	Sample (ml)	Remark(s)
		Hour	Min			1	2	3	Ave.				
12.45	20190219	0		200	241	0.069	0.074	0.081					R0 pH 5.7
13.15				-	242	0.095	0.095	0.093					R1
13.50				-	242	0.115	0.111	0.112					R2
14.00				200	243	0.151	0.151	0.145					R3
14.30				199	244	0.232	0.237	0.228					R4 pH 5.5
15.00				198	248	0.041	0.040	0.040		10			R5
15.30				194	254	0.067	0.068	0.074		10			R6
16.00				192	267	0.130	0.141	0.125		10			R7
16.30				190	283	0.205	0.200	0.191		10			R8
17.00				183	316	0.324	0.349	0.355		10			R9
17.30				180		0.040	0.041	0.042		100			R10
18.00				174		0.046	0.049	0.050		100			R11
20.00				168	455	0.120	0.121	0.121		50			R12
20.30				165		0.118	0.115	0.117		50			

Forsik 5 RIGHT

Batch code: MR Batch type: DSM17938 pH 5.5 Date: 20190219 Carbon source: Maltose
 Nitrogen source: - Sparging gas: - Stirrer speed: 100 Working volume: 1L
 GC sample code: - Operator: - Fermenter code: Applikon 2

Protocol	Date	Time		%w/v KOH	%CO ₂ Osmos	OD ₆₀₀				df	Abs OD ₆₀₀	Sample (ml)	Remark(s)
		Hour	Min			1	2	3	Ave.				
12.45	20190219			50	244	0.087	0.090	0.093					R0 pH 5.7
13.15				-	245	0.110	0.108	0.108					R1
13.50				-	245	0.133	0.130	0.135					R2
14.00				50	247	0.189	0.195	0.181					R3
14.30				49	248	0.318	0.292	0.316					R4 pH 5.5
15.00				48	251	0.051	0.057	0.049		10			R5
15.30				46	258	0.090	0.086	0.087		10			R6
16.00				41	294	0.140	0.138	0.132		10			R7
16.30				38	291	0.224	0.237	0.227		10			R8
17.00				31	312	0.574	0.392	0.365		10			R9
17.30				28-30		0.037	0.035	0.040		100			R10
18.00				44		0.040	0.037	0.035		100			R11
20.00				27	483	0.130	0.131	0.130		50			R12
20.30				21		0.122	0.124	0.125		50			

FORSØK 8 LEFT

Batch code: SF Batch type: DSM 17938 pH 5.5 Date: 20190314 Carbon source: SUCROSE + FRUCTOSE
 Nitrogen source: - Sparging gas: - Stirrer speed: 100 Working volume: 1L
 GC sample code: - Operator: KB Fermenter code: Applikon 1

Protocol	Date	Time		pH	DO	OD ₆₀₀				df	Abs OD ₆₀₀	Sample (ml)	Remark(s)
		Hour	Min			1	2	3	Ave.				
12.00	20190314			200	568	0.104	0.098	0.095					
12.30				200	568	0.131	0.127	0.128					
13.00				199	568	0.188	0.183	0.191					NBCC pnu saltnes
13.30				-	-	0.350	0.370	0.338	0.355				
13.30				198	570	0.056	0.052	0.052					
14.00				-	583	0.119	0.116	0.118					
14.30				187	540	0.206	0.209	0.200					
-				-	-	0.069	0.071	-					
15.00				184	613	0.036	0.034	0.034				100	
15.30				-	685	0.040	0.042	0.049				100	
16.00				-	698	0.043	0.050	0.046				100	
16.30				-	634	0.044	0.044	0.046				100	
17.00				174	721(?)	0.046	0.044	0.044				100	
18.45				166	729	0.061	0.080	0.081				50	

FORSØK 8 RIGHT

Batch code: SF Batch type: DSM 17938 pH 5.5 Date: 20190314 Carbon source: SUCROSE + FRUCTOSE
 Nitrogen source: - Sparging gas: - Stirrer speed: 100 Working volume: 1L
 GC sample code: - Operator: KB Fermenter code: Applikon 2

Protocol	Date	Time		pH	DO	OD ₆₀₀				df	Abs OD ₆₀₀	Sample (ml)	Remark(s)
		Hour	Min			1	2	3	Ave.				
12.00	20190314			50	529	0.101	0.107	0.107					
12.30				50	530	0.139	0.141	0.135					
13.00				49	533	0.213	0.214	0.225					NBCC pnu saltnes
13.30				47	533 (2.053)	0.345	0.256	0.257				10	
14.00				-	546	0.137	0.133	0.144				10	
14.30				38	556	0.245	0.240	0.245				10	
15.00				34	580	0.037	0.039	0.037				100	
15.30				-	608	0.051	0.049	0.043				100	
16.00				-	619	0.052	0.051	0.052				100	
16.30				-	621	0.043	0.045	0.043				100	
17.00				19-50	638	0.044	0.049	0.042				100	
18.45				42	719	0.079	0.080	0.078				50	